PHYSICAL REVIEW B **79**, 161304(R) (2009)

# Dielectric screening versus quantum confinement of phosphorus donors in silicon nanocrystals investigated by magnetic resonance

R. N. Pereira,[1,2,*] A. R. Stegner,[1] T. Andlauer,[1] K. Klein,[1] H. Wiggers,[3] M. S. Brandt,[1] and M. Stutzmann[1]
[1]*Walter Schottky Institut, Technische Universität München, Am Coulombwall 3, 85748 Garching, Germany*
[2]*Departamento de Física and I3N, Universidade de Aveiro, 3810-193 Aveiro, Portugal*
[3]*Institut für Verbrennung und Gasdynamik, Universität Duisburg-Essen, 47048 Duisburg, Germany*
(Received 20 February 2009; published 16 April 2009)

We monitor the localization of donor wave functions when going from the bulk to nanoscales by electrically detected magnetic resonance of P-doped Si nanocrystal networks. Analysis of the P hyperfine splitting shows that for nanocrystals with radii above ~6 nm donor localization is dominated by a reduction in dielectric screening relative to the bulk rather than by quantum confinement. Screening effects become negligible only for radii below ~2 nm, where quantum confinement dominates. Thus, hyperfine interactions can serve as sensitive probes to study basic properties of doped nanocrystals and provide data to critically test theoretical models.

DOI: 10.1103/PhysRevB.79.161304 PACS number(s): 78.67.Bf, 76.30.−v, 85.40.Ry

Semiconductor nanocrystals (NCs) are the basis for new generations of devices.[1–3] The recently developed capability of producing macroscopic amounts of freestanding Si-NCs (Refs. 4 and 5) has opened up the route for applications such as cost-effective large area electronics using printable Si inks[6] or high-efficiency solar cells,[7] where properties are tailored via electronic doping at nanoscales, a process quite distinct from the bulk.[8–11] Underlying mechanisms such as dopant confinement, which also influences doping efficiency, are the subject of intense debate. Available experimental data so far have been explained only on the basis of quantum confinement imposed by confining surface potentials,[10,12] though it has been proposed by theory that dopant localization can also result from a decrease of dielectric screening (dielectric confinement).[13] Here, we report the experimental observation of the contribution of dielectric confinement to dopant localization in NCs. We monitor dopant wave functions when going from bulk to nanoscales and compare the data with a theoretical model which, unlike previous first-principles approaches, can be applied to very large NCs and accounts for quantum and dielectric confinement separately.

Phosphorus donors in bulk crystalline Si (*c*-Si) are conventionally described as a hydrogenic impurity, where the donor-electron potential energy is given by the electrostatic potential of the singly-charged impurity ion screened by the bulk dielectric constant $\varepsilon_{\text{bulk}}=11.7$. The donor-electron ground-state envelope function is the 1*s* state of a hydrogenlike atom with an effective Bohr radius $a^*_{\text{bulk}}=1.67$ nm,[14] as shown schematically in Fig. 1(a). The electron probability density at the P nucleus $|\Psi(0)|^2$ can be probed with electron paramagnetic resonance (EPR) via the Fermi contact hyperfine splitting (hfs) $A \propto |\Psi(0)|^2$ arising from interaction between the electron spin and the $^{31}$P nucleus spin $I=1/2$, which in *c*-Si is $A_{\text{bulk}}=4.2$ mT.[15] It is observed that the hfs of donors in NCs increases with respect to the bulk, which has been explained on the basis of quantum confinement models, assuming that donor wave-function localization is due to the confining potential barrier $V_0$ of the surrounding medium.[10,12] Namely, the dependence of the hfs associated with P in Si-NCs embedded in amorphous $SiO_2$ on NC radius $R$ was described with a $R^{-3}$ law,[12] which corresponds to an electron in a spherical potential of infinite height,[16] neglecting the Coulomb potential. A more elaborate quantum confinement approach was applied to describe hfs changes observed for Li donors in ZnO NCs.[10] Here, the donor electron is confined by $V_0$ and experiences the Coulomb potential of the Li nucleus screened by $\varepsilon_{\text{bulk}}$. In quantum confinement models, the donor wave function deviates strongly from the hydrogenlike function due to influence of $V_0$, as schematically shown in Fig. 1(b). However, recent first-principles pseudopotential calculations have concluded that P donors in

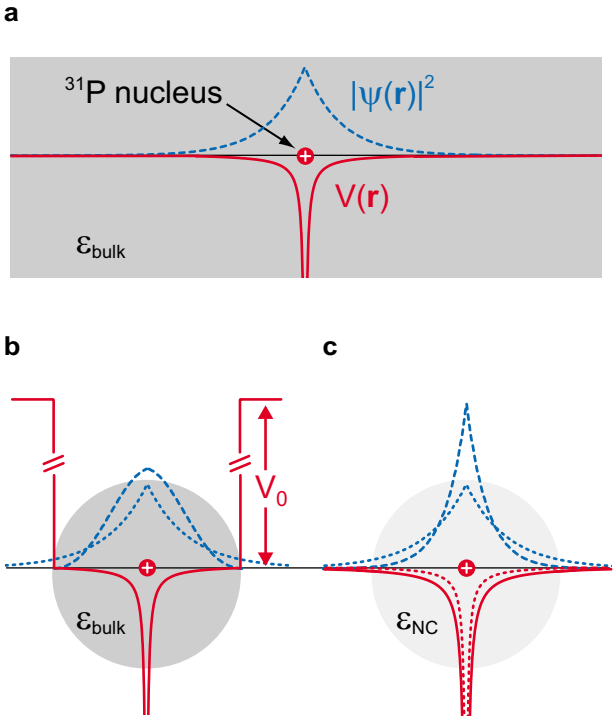


FIG. 1. (Color online) (a) Hydrogenlike model of a donor impurity in a bulk semiconductor. (b) Quantum confinement and (c) dielectric confinement models of a donor impurity in a semiconductor NC. Dashed and solid traces represent electron probability density $|\Psi(r)|^2$ and potential energy $V(r)$, respectively. Dotted traces in (b) and (c) correspond to the bulk situation.

 

Si-NCs can be very well described by a hydrogenic system with the effective Bohr radius decreasing continuously as the NC size is reduced.[17,18] This implies that the donor-electron potential energy should be well described simply by the impurity nucleus Coulomb potential and $V_0$ does not contribute significantly to donor localization. In a pure dielectric confinement model, donor localization could arise from a NC size-dependent screening of the impurity Coulomb potential, described by a NC size-dependent screening dielectric constant $\varepsilon_{NC}(R)$. A reduction in the Coulomb potential screening in NCs with respect to the bulk has been predicted in several theoretical studies,[13,19–21] which leads to a decrease in the hydrogenic Bohr radius and to an increase in electron density at the impurity nucleus $|\Psi(0)|^2$, as shown in Fig. 1(c). Dielectric screening effects have been completely neglected when describing experimental data. A hfs dependence scaling as $R^{-1.5}$ was suggested from a power-law fitting to the *ab initio* data obtained for small NCs ($R \leq 1.1$ nm),[18] in clear contrast to the $R^{-3}$ dependence of quantum confinement models. Hence, different studies assume very distinct scenarios, and the relative contributions of dielectric and quantum confinement are controversial. To clarify this, we measure the continuous increase of the hfs of P donors when going from the bulk to Si-NCs with $R \sim 3$ nm. Although conventional EPR is the method of choice for studying donor states, its application in NCs is often limited by a lack of sensitivity.[22] We overcome this difficulty by using electrically detected magnetic resonance (EDMR) of P-doped Si-NC networks.

Freestanding P-doped Si-NCs with mean particle $R$ in the range 3–18 nm, as measured by the Brunauer-Emmet-Teller technique, were produced by microwave-induced decomposition of $SiH_4$ and $PH_3$.[4,22] Si-NCs have a log-normal size distribution with a standard deviation of the radius natural logarithm of typically $\sigma=0.40$.[4] P doping was $0.1-5 \times 10^{20}$ cm$^{-3}$, defined as the atomic density of $c$-Si multiplied by the $PH_3$ fraction in the total precursor gases flow. EDMR samples consisted of films of densely packed H-terminated Si-NCs on polyimide substrates, as described in Ref. 22. EDMR was carried out under sample illumination (Schott KL1500LCD cold light source) at ~7 K in a He flow cryostat using a cw $X$-band EPR spectrometer with a $TM_{110}$ cavity (magnetic field modulation amplitude and frequency were 0.12 mT and 2 kHz). Spectra were recorded with an applied bias field of $10^5$ V cm$^{-1}$, resulting in currents of 0.01–1 $\mu$A. For EDMR detection, we use a two-channel lock-in amplifier where both the signal ($S_{0^\circ}$) in-phase with the field modulation and the component phase-shifted by 90° ($S_{90^\circ}$) are detected. From these signals, we calculate the EDMR spectrum corresponding to any lock-in phase-shift setting $\Delta\theta$ with the expression $S_{0^\circ}\cos\Delta\theta - S_{90^\circ}\sin\Delta\theta$. Since in EDMR different states usually participate in spin-dependent processes with distinct dynamics, these can be separated via their dependence on the lock-in phase setting.[23] Here, we analyze spectra corresponding to a $\Delta\theta$ that maximizes the relative intensity of P hyperfine lines.

Electronic-state calculations of P in Si-NCs were performed using a continuous medium model assuming a single-band effective mass, with the P nucleus represented by a positive charge at the center of a spherical NC. The donor-electron Hamiltonian operator is given by

$$\mathcal{H}(\mathbf{r}) = \frac{\mathbf{p}^2}{2\hat{m}^*} + V(r), \tag{1}$$

where $\mathbf{p}$ is the donor-electron momentum operator, $r$ is the distance from the donor nucleus, and $\hat{m}^*$ denotes the effective $3\times3$ mass tensor for a Si $\Delta$ valley with longitudinal and transverse masses of $m_l=0.92m_0$ and $m_t=0.19m_0$, respectively ($m_0$ is the free-electron mass). $V(r)$ is the donor-electron potential energy, including the Coulomb interaction and surface confining potential $V_0$. To compare calculated hfs with experimental values, we have to include the so-called central-cell correction $W(r)$, describing the potential very close to the donor nucleus.[24] We use the $W(r)$ parametrization established for P in $c$-Si.[24,25] The Hamiltonian was solved on a real-space grid using the nextnano$^{++}$ code.[26] The hfs $A(R)$ was calculated from the relative change of the electron probability density at the donor nucleus with respect to the bulk $A(R)=A_{bulk}|\Psi(0)|^2/|\Psi(0)_{bulk}|^2$. The bulk wave function $\Psi(r)_{bulk}$ results from calculation in a NC with $R=25$ nm. To avoid the $r=0$ singularity, potentials were replaced by $-Q\delta_{\mathbf{r},0}$ for the central grid node, following Ref. 25 ($\delta_{\mathbf{r},0}$ is the Kronecker delta). The parameter $Q$ was fitted to obtain the experimental binding energy of P in $c$-Si (45.6 meV), i.e., a NC with $R=25$ nm.

In a recent study of P-doped Si-NCs, a P-related line, denoted hf($^{31}$P), was observed 2 mT above $g=1.998$ for $R \sim 15$ nm.[22] The observed shift of 2 mT indicates that this line corresponds to the high-field resonance of the hyperfine doublet of isolated P in Si-NCs.[22] This resonance is due to spin-dependent recombination, a promising electrical readout path of $^{31}$P spin states.[27] To measure donor wave-function localization and accurately monitor its dependence on NC size, we take advantage of the EDMR detection phase sensitivity to resolve both the low-field and high-field resonances of the P hyperfine doublet. Figure 2 shows EDMR spectra recorded with P-doped Si-NCs with different mean sizes for $\Delta\theta \sim 80^\circ$.

The strongest feature in each spectrum located at $g \simeq 2.006$ is due to different configurations of Si dangling bonds.[22] For the 14 nm sample, in addition to the high-field hf($^{31}$P) line, another resonance is revealed as a shoulder on the left side of the defect-related line, which we attribute to the low-field hf($^{31}$P) line. The hf($^{31}$P) line splitting of about 4.2 mT and their median at $g=1.998$ are typical for substitutional P in $c$-Si.[28] In spectra of smaller NCs, the low-field hf($^{31}$P) line shifts to lower resonance fields, whereas the corresponding high-field hf($^{31}$P) line shifts to higher fields. The center position of the hf($^{31}$P) lines remains constant at $g \sim 1.998$. This corroborates the assignment of these lines to isolated substitutional P inside the Si-NCs, with the observed hfs increase originating from an enhanced wave-function localization. Figure 2 shows that the hf($^{31}$P) lines become broader and asymmetric when the NCs size is decreased. To verify that these effects are due to the NCs size distribution, we simulated the expected line shapes taking into account the known log-normal size distribution $D(R;R_0,\sigma)$ of our samples and the hfs size dependence $A(R) \propto R^{-1.5}$ proposed from pseudopotential studies.[18] To this end, we use the convolution

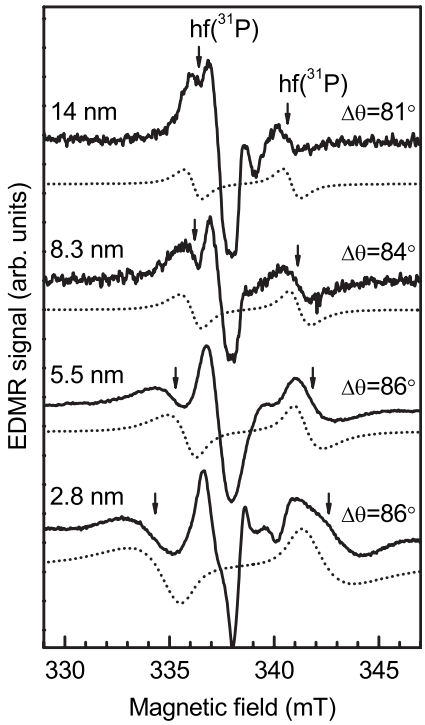


FIG. 2. EDMR spectra of P-doped Si-NCs with 14 to 2.8 nm mean radii for $\Delta\theta \sim 80°$ (solid traces). Due to the detection method, spectra show first derivatives of the resonant current changes. Dotted traces depict simulated hf($^{31}$P) line shapes.

$$\int_0^\infty D(R;R_0,\sigma)[L(B;\Gamma,B_-)+L(B;\Gamma,B_+)]dR, \qquad (2)$$

where $R_0$ is the sample mean NC radius and $L(B;\Gamma,B_\pm)$ are Lorentzian line shapes with center magnetic field positions $B_\pm = h\nu/g\mu_B \pm A(R)/2$ ($h$ is the Planck constant, $\nu$ is the microwave frequency 9.467 GHz, $\mu_B$ is the Bohr magneton, and $g=1.998$ is the $g$ factor for P in $c$-Si.[28]) As full width at half maximum, we use the value $\Gamma=1.3$ mT observed for the high-field hf($^{31}$P) line in the 14 nm sample spectrum. As seen in Fig. 2, the simulated lines reproduce the experimental observations quite well. Since the simulated spectra were calculated using independently determined parameters, this gives further support to our assignment of hf($^{31}$P) lines to isolated P.

In Fig. 3, the hfs size dependence, indicated by arrows in Fig. 2, is shown. A power-law fitting to the data gives a dependence of $R^{-1.3}$ (not shown), in close accordance with the $R^{-1.5}$ dependence proposed in *ab initio* studies.[18] In Fig. 3, our data are compared with data from an earlier EPR study of Si-NCs embedded in $a$-$SiO_2$ in the radius range of 1.5–3.5 nm.[12] The $A(R) \propto R^{-3}$ dependence (dashed trace) used to describe these previous results,[12] assuming a pure quantum confinement model, clearly deviates from our data.

Here, we use an approach that considers both the surface confining potential and a NC size-dependent screening of the Coulomb interaction between the P nucleus and donor electron. A decrease in the screening of the Coulomb potential of hydrogenlike systems in NCs with respect to the bulk has

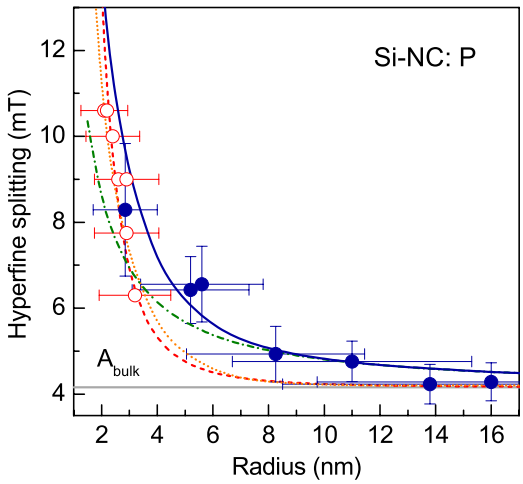


FIG. 3. (Color online) Experimental dependence of $^{31}$P hfs on NCs mean radius (filled circles), together with the dependencies obtained from the (i) quantum confinement model (dotted trace), (ii) dielectric confinement model (dash-dotted trace), and (iii) full model (solid trace). The EPR hfs (open circles) and corresponding fitting with a $R^{-3}$ law (dashed trace) reported by Fujii *et al.* (Ref. 12) for Si-NCs embedded in $a$-$SiO_2$ are also shown. Horizontal and vertical error bars represent the size distribution interval that contains 70% of the NCs and the peak-to-peak width of the high-field hf($^{31}$P) resonance, respectively. The horizontal gray line indicates the value $A_{\text{bulk}}$.

been predicted using empirical pseudopotentials,[13] phenomenological calculations,[20] self-consistent linear combinations of atomic orbitals,[19] and *ab initio* methods.[21] In these studies, the Coulomb screening dependence on NC size has been described by a size-dependent screening dielectric constant $\varepsilon_{\text{NC}}(R)$, parameterized using a generalization of the Penn model to NCs, i.e., $\varepsilon_{\text{NC}}(R)=1+(\varepsilon_{\text{bulk}}-1)/[1+(\alpha/R)^l]$. As already noted by Wang and Zunger,[13] the screening dielectric constant $\varepsilon_{\text{NC}}(R)$ is defined for the specific case of screening of the Coulomb potential of a hydrogenlike system, and it is not directly comparable with other definitions of NC dielectric constants.[29,30] In our model, the donor-electron potential energy is then given by $V(r)=-e^2/\varepsilon_{\text{NC}}(R)r+W(r)$ for $0<r \leq R$ and for $r>R$ is given by a hard wall confining potential $V_0=+\infty$. We use the parameters $\alpha=0.97$ nm and $l=1.3$ obtained by Öğüt *et al.*[21] Use of values $\alpha$ and $l$ obtained by other authors gives practically the same results. As can be seen in Fig. 3, the results of our model (solid trace) describe very well both our experimental data and the previously reported data, with at most a small discrepancy observed for the data point corresponding to the largest NC size analyzed by Fujii *et al.*,[12] possibly due to the different methods used for NC size determination. To understand the relative contributions of quantum confinement and dielectric screening, we considered two additional variations of the model: (i) pure quantum confinement, where the dielectric-screening size dependence is neglected by substituting $\varepsilon_{\text{NC}}(R)$ with $\varepsilon_{\text{bulk}}$ (dotted trace) and (ii) pure dielectric confinement, where the confining surface potential is neglected ($V_0=0$, dash-dotted trace). As seen in Fig. 3, the quantum confinement model predicts a much lower hfs than that observed experimentally

for Si-NCs with radii down to ~3 nm, demonstrating that quantum confinement alone cannot account for the observed donor localization in this size range. However, the dielectric confinement model gives a good description of the data for Si-NCs with radii down to 6 nm.

Our model does not consider donor-electron interaction with image charges on the NC surface associated with the impurity ion and the donor electron (self-polarization).[19,25] For a central donor position, the ion image charge adds the term $-e^2/R(1-1/\varepsilon_{NC})$ to the potential energy.[19] This is independent of $r$ and, therefore, does not alter the donor wave-function shape and hfs. We performed calculations where the self-polarization term was added to our model using the expression given in Ref. 25 and found that this leads to a negligible increase of the calculated hfs. Although our model assumes P only at the NC center, this should not affect our conclusions. According to *ab initio* studies, the hfs of off-center P varies only within ~10% of its value for the central P position and a significant decrease is predicted only for P in the close vicinity of the surface.[17] We expect a negligible contribution of these sites to P hyperfine spectra since for NC sizes investigated here, they represent only less than 15% of the total number of sites. We should also note that a large contribution of these surface sites would lead to NC size dependencies of the hfs and hf($^{31}$P) line shape different from those observed here, which as discussed above agree with the $R^{-1.5}$ dependence estimated theoretically for central P.[18] During growth, a segregation of P to the Si-NCs surface occurs.[31,32] However, after oxidation in air and subsequent removal of the oxide, these surface P states are largely removed.[22] We note that our experimental data and analysis do not support a screening dielectric constant inside the NCs equal to $\epsilon_{bulk}$, which has been assumed in some theoretical studies,[30,33] in disagreement with Refs. 13 and 19–21. Such hypothesis is also incompatible with recent *ab initio* calculations that concluded that P donors in Si-NCs can be well described by a hydrogenlike system with the effective Bohr radius decreasing continuously as the nanocrystal size is reduced,[17,18] which implies that the impurity Coulomb potential increases with decreasing NC size.[17]

In summary, a strong localization of donor states is already observed for NCs considerably larger than predicted by quantum confinement. Three NC size regimes are found: for $R > 3.5a^*_{bulk}$, donor localization is determined by a decrease in dielectric screening of the impurity Coulomb potential, whereas for $R < a^*_{bulk}$, the confining surface potential dominates. For intermediate NC sizes, both dielectric and quantum confinement have a sizeable contribution to donor-electron wave-function localization.

Financial support from the EU (PSYNANO), DFG (Contract No. SFB 631, GK 1240), Evonik Degussa S2B Nanotronics, and the state of North Rhine-Westfalia is acknowledged.

*rnpereira@ua.pt

[1] W. Lu and C. M. Lieber, Nature Mater. **6**, 841 (2007).
[2] G. Hodes, Adv. Mater. (Weinheim, Ger.) **19**, 639 (2007).
[3] Y. Sun and J. A. Rogers, Adv. Mater. (Weinheim, Ger.) **19**, 1897 (2007).
[4] J. Knipping *et al.*, J. Nanosci. Nanotechnol. **4**, 1039 (2004).
[5] L. Mangolini *et al.*, Nano Lett. **5**, 655 (2005).
[6] L. Mangolini and U. Kortshagen, Adv. Mater. (Weinheim, Ger.) **19**, 2513 (2007).
[7] M. C. Beard *et al.*, Nano Lett. **7**, 2506 (2007).
[8] D. J. Norris *et al.*, Nano Lett. **1**, 3 (2001).
[9] S. C. Erwin *et al.*, Nature (London) **436**, 91 (2005).
[10] S. B. Orlinskii, J. Schmidt, E. J. J. Groenen, P. G. Baranov, C. de Mello Donega, and A. Meijerink, Phys. Rev. Lett. **94**, 097602 (2005).
[11] D. J. Norris *et al.*, Science **319**, 1776 (2008).
[12] M. Fujii, A. Mimura, S. Hayashi, Y. Yamamoto, and K. Murakami, Phys. Rev. Lett. **89**, 206805 (2002).
[13] L. W. Wang and A. Zunger, Phys. Rev. Lett. **73**, 1039 (1994).
[14] M. Stutzmann, D. K. Biegelsen, and R. A. Street, Phys. Rev. B **35**, 5666 (1987).
[15] G. Feher, Phys. Rev. **114**, 1219 (1959).
[16] J. H. Davies, *The Physics of Low-Dimensional Semiconductors - An Introduction* (Cambridge University Press, Cambridge, UK, 2006).
[17] T. L. Chan *et al.*, Nano Lett. **8**, 596 (2008).
[18] D. V. Melnikov and J. R. Chelikowsky, Phys. Rev. Lett. **92**, 046802 (2004).
[19] M. Lannoo, C. Delerue, and G. Allan, Phys. Rev. Lett. **74**, 3415 (1995); G. Allan, C. Delerue, M. Lannoo, and E. Martin, Phys. Rev. B **52**, 11982 (1995).
[20] R. Tsu *et al.*, Mater. Res. Soc. Symp. Proc. **283**, 437 (1993).
[21] S. Öğüt, J. R. Chelikowsky, S. G. Louie, Phys. Rev. Lett. **79**, 1770 (1997).
[22] A. R. Stegner, R. N. Pereira, K. Klein, R. Lechner, R. Dietmueller, M. S. Brandt, M. Stutzmann, and H. Wiggers, Phys. Rev. Lett. **100**, 026803 (2008).
[23] H. Dersch, L. Schweitzer, and J. Stuke, Phys. Rev. B **28**, 4678 (1983).
[24] S. T. Pantelides and C. T. Sah, Phys. Rev. B **10**, 621 (1974).
[25] V. A. Belyakov and V. A. Burdov, Phys. Rev. B **76**, 045335 (2007).
[26] S. Birner *et al.*, IEEE Trans. Electron Devices **54**, 2137 (2007).
[27] A. R. Stegner *et al.*, Nat. Phys. **2**, 835 (2006).
[28] P. R. Cullis and J. R. Marko, Phys. Rev. B **11**, 4184 (1975).
[29] C. Delerue, M. Lannoo, and G. Allan, Phys. Rev. B **68**, 115411 (2003).
[30] A. Franceschetti and M. C. Troparevsky, Phys. Rev. B **72**, 165311 (2005).
[31] X. D. Pi *et al.*, Appl. Phys. Lett. **92**, 123102 (2008).
[32] R. Lechner *et al.*, J. Appl. Phys. **104**, 053701 (2008).
[33] F. Trani, D. Ninno, G. Cantele, G. Iadonisi, K. Hameeuw, E. Degoli, and S. Ossicini, Phys. Rev. B **73**, 245430 (2006).